

PACS №: 84.90.+a; 77.90.+k

G. Staines\*, Helmut Hofmann\*, Josef Dommer\*,

L.L. Altgilbers\*\*, Ya. Tkach\*\*\*

\*Diehl Munitionssysteme GmbH & Co. KG,

Nuremberg, Germany

\*\*U.S. Army Space and Missile Defense Command,

Huntsville, AL, 35807

\*\*\*Gomez Research Associates,

Huntsville, Al

# Compact Piezo-Based High Voltage Generator - Part I: Quasi-Static Measurements

## Contents

1. Introduction	373
2. Piezo-Based HVG Mathematical Theory	374
3. Results and Discussion	377
4. Conclusions	382

## Abstract

This paper presents the results of an effort to develop and test a piezo-based high voltage generator (HVG). A theoretical model was developed and, in order to verify this model, quasi-static measurements were conducted using a 15 mm diameter and 20 mm long cylindrical PZR-5A piezoelectric element and an electric press driven by a rotating screw. Measurements were made using various load capacitances and resistances and using single and multiple piezo elements. The results of these measurements will be presented. A prototype piezo-based HVG with a diameter of 65 mm and a length of 275 mm was also built and tested and the results will be presented in a follow-on paper. This generator produced almost 400 kV with 3 J of energy stored in the generator.

## 1. Introduction

Piezoelectric generators (PEGs) are simple, inexpensive, and very compact devices. Unlike other explosive power sources, such as magnetocumulative or ferromagnetic generators, PEGs do not require the use of explosives to produce the required mechanical forces to generate electrical power. However, they are inherently low-energy devices with a maximum energy density of only about  $1 \text{ J/cm}^3$ , which limits their utility to certain specific applications.

To the best of the authors knowledge, work on explosive driven PEGs can be traced back to the early 1960s in the United States [1–5], Former Soviet Union [6–7], and France [8]. All of these early studies had two central themes: using ferroelectric or piezoelectric materials as the working body and using shock waves to depolarize these materials.

Most of the early studies focused on either single crystals or ferroceramic materials such as barium titanate, Tibalit, lithium niobate, and lead zirconate titanate (PZT). These materials are still investigated today, but there is also interest in ferroelectric polymers such as PVDF.

One of the early papers that investigated the feasibility of using PEGs as pulsed power supplies was by J.E. Beasancon, J. David, and J. Vedel [8]. Since then, others have investigated their utility as pulsed power devices including A.B. Prishchepenko [9], B.M. Novac [10], S. Shkuratov [11], and Ya. Tkach [12].

A.B. Prishchepenko and his team [9] probably have the most experience with PEGs with work beginning in 1983 and continuing through the late 1990s. They have used their PEGs to drive capacitive loads and in conjunction with ferromagnetic generators.

It was first observed by B.M. Novac et al. [10] that

these generators work best when the shock pressures are dampened. They investigated the influence of pressure loading on PZT and found that when the pressure exceeded 50 kbar, the output current dramatically decreased. They theorized that this is caused by internal short circuiting of the generator due to massive generation of electrical charges. Two types of attenuators were used in their experiments: copper-Plexiglas and steel.

In this study, it was decided to determine the optimal pressures for PEG operation and it was found that shock pressures are detrimental since they cause the ceramics to fracture and can induce electrical breakdown. Therefore, one of the results of this study was to determine if propellants, rather than explosives, could be efficiently used to generate high voltages from these generators. The results of these investigations are presented.

## 2. Piezo-Based HVG Mathematical Theory

The first step in the development process was to verify the characteristics of the cylindrical PZT-5A piezo element selected for the HVG. The simplest and most compact method of obtaining high voltage from the piezo was to compress it axially. The compression was quasi-static, so that the dynamic mechanical processes need not be considered. PZT-5A is a lead zirconate titanate polycrystalline ceramic material [13] that is commonly used in igniters in which voltages as high as 20 kV are produced. Large PZT elements were used in order to maximize the available charge, and hence, output voltage, and to account for possible charge leakage during the relatively slow compression process.

The constitutive equations are

$$S_j = s_{kj}^E T_k + d_{im} E_m, \quad (1)$$

$$D_i = d_{im} T_m + \varepsilon^T E_m, \quad (2)$$

or equivalently

$$S_j = s_{kj}^D T_k + g_{nj} D_n, \quad (3)$$

$$E_n = \beta_{mn}^T D_m - g_{nj} T_j, \quad \beta_{mm} = \varepsilon_{mm}^{-1}, \quad (4)$$

where  $s^D$  is the open-circuit compliance defined by

$$s^D = s^E - d_{jk} d_{mi} (\varepsilon_{mj}^T)^{-1} \quad (5)$$

$\vec{g}$  is the piezoelectric voltage coupling,  $\vec{d}$  contains the piezoelectric coupling terms which relate the electrical and mechanical properties of the material,  $\vec{S}$  is the strain (dimensionless),  $\vec{D}$  is the electric displacement or charge density (C/m<sup>2</sup>),  $\vec{E}$  is the electric field (V/m), and  $\vec{T}$  is the applied stress (N/m<sup>2</sup>).

Considering the simple case of a cylindrical piezo element, which is compressed axially in the  $z$ -direction, there are two cases of specific interest. The

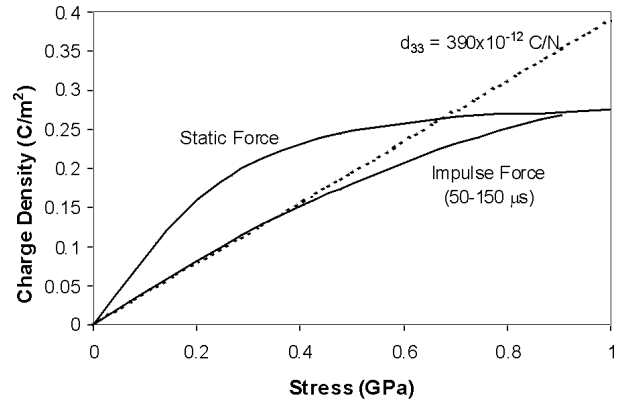


Fig. 1. Charge produced from short-circuited PZT-5A piezo element [14].

first is when the electrodes at each end of the element are short-circuited together. In this case,  $E_3 = 0$  and the charge produced by the piezo element can be calculated readily from Eq. (2):

$$Q = D_3 A = d_{33} T_3 A = d_{33} F, \quad (6)$$

where  $F$  is the applied force,  $A$  is the cross-sectional area of the element, and the subscripts refer to the location in the respective matrices. Note that the force cannot be increased indefinitely due to a nonlinear piezoelectric effect in the short circuit case, which can lead to irreversible depolarization of the piezo element. This effect occurs when the mechanical stresses in the piezo element are sufficient to cause changes in the ferroelectric domain boundaries. The influence of this nonlinear effect is shown in Fig. 1, which is reproduced from [14]. When the applied stress is an impulse with duration of 50–150  $\mu$ s, the charge produced by the piezo element increases linearly with stress according to the linear theory discussed above. As the stress increases, less charge is produced than predicted by theory. The maximum charge density which can be generated is about 0.275 C/m<sup>2</sup>. The extent of depolarization is dependent on the duration of the applied stress. If the stress is applied on a time scale much shorter than the relaxation time of the domains, the depolarization is inhibited. For the static case, the nonlinear effect produces more current than predicted at lower stresses. Once a PZT-5A element has produced a charge density of 0.275 C/m<sup>2</sup>, as for the dynamic case, it is almost completely irreversibly depolarized. However, it should be noted that for single use applications, the maximum charge produced by either static or dynamic stresses are the same. Since static stresses of 0.5 GPa are readily achievable, quasi-static operation of the piezo HVG is feasible and offers similar performance to more mechanically complicated concepts which exploit impulsive stressing of the piezo.

From Eq. (1) the longitudinal strain for the short-

circuit case is simply

$$\frac{\Delta l}{l} = S_3 = s_{33}^E T_3 \quad (7)$$

where  $l$  is the length of the piezo element. For instance, a stress of 100 MPa will produce a strain of about 0.2 %. This is small and shows that a piezo HVG using static stressing will effectively contain no moving components, a further advantage relative to reliability and compact design.

The other case of interest is when the electrodes are open-circuit, so that no charge displacement is possible and  $D_3 = 0$ . The voltage  $V$  developed across the piezo when the force is applied can be calculated using Eq. (4).

$$V = E_3 l = -g_{33} T_3 l = -g_{33} \frac{Fl}{A} = -\frac{d_{33} F}{C_0} \quad (8)$$

where  $C_0$  is the capacitance of the unstressed piezo element. Note that for a PZT-5A cylinder 15 mm in diameter and 20 mm long, a force of 10 kN produces a voltage of 28 kV. For a given maximum stress  $T_3$ , the voltage depends only on the material constant  $g_{33}$  and the length of the piezo. The open-circuit voltage increases in proportion with the length of the piezo element.

A very important consideration for the open-circuit case is that since the electric field is aligned with the polarization vector, the depolarization effect discussed in relation to the short-circuit case does not appear in the open-circuit case. This means that if the quasi-static force is applied on a timescale sufficiently short that leakage current does not discharge the piezo prematurely, then the voltage will continue to increase linearly with stress up to the point at which the piezo element shatters. From [14], the maximum compressive stress that can be tolerated by PZT-5A is at least 600 MPa. For a 20 mm long piezo element, this corresponds to an open-circuit voltage of 300 kV. This is exceptionally high and certainly enough for driving some loads. Note however that this value will only be achieved provided the leakage current does not prematurely discharge the piezo element. In practice, even 100 kV would be adequate in some applications.

Note that from Eq. (8), the charge on the ends of the piezo cylinder is

$$Q = C_0 V = -d_{33} F = -\varepsilon_{33}^T g_{33} F. \quad (9)$$

Thus, the amount of charge depends only on the material properties and the applied force. The advantage of using thicker piezos follows from the fact that for a given maximum stress, they can withstand higher force since the cross-sectional area is larger.

The axial strain can be calculated from Eqs. (4) and (5):

$$\frac{\Delta l}{l} = S_3 = s_{33}^D T_3 = \left( s_{33}^E - \frac{d_{33}^2}{\varepsilon_{33}^T} \right) \frac{F}{A}. \quad (10)$$

A final parameter of significant interest for the open-circuit case ( $D_3 = 0$ ) is the maximum electrical energy stored in the piezo. If the total energy  $U_D$  stored in the element is the sum of the electrostatic energy  $U_e$  and the mechanical energy  $U_m$  used to deform the element, then

$$U_D = U_m + U_e. \quad (11)$$

The total energy must be equal to the input mechanical energy, so that

$$U_D = \frac{\nu}{2} s_{33}^D T_3^2, \quad (12)$$

where  $\nu$  is the volume of the piezo element. The electromechanical coupling coefficient is used to determine the proportion of the total piezo energy contained in the electric field. Specifically, the factor  $k^2$  is the ratio of the stored electrical energy to the total energy. For a cylindrical piezo element, the most important quantity is the longitudinal coupling factor, which is related to the various factors discussed previously by

$$k_{33}^2 = \frac{d_{33}^2}{s_{33}^E \varepsilon_{33}^T}. \quad (13)$$

Therefore,

$$U_e = \frac{\nu}{2} k_{33}^2 s_{33}^D T_3^2. \quad (14)$$

Using Eqs. (5),(8),(13), and (14), the following expression is obtained for the electrical energy:

$$U_e = \frac{1}{2} \varepsilon_{33}^T (1 - k_{33}^2) \frac{A}{l} V^2 = \frac{1}{2} (1 - k_{33}^2) C_0 V^2, \quad (15)$$

where  $C_0$  is the capacitance of the unstressed piezo element. This capacitance can be calculated from

$$C_0 = \varepsilon_{33}^T \frac{A}{l}. \quad (16)$$

For a PZT-5A cylinder with a diameter of 15 mm and a length of 20 mm, a value of 133 pF is obtained using Eq. (16). This compares well with a measured value of 135 pF. Note that in applications such as gas igniters, it is possible, in principle, to recover the mechanical energy used to compress the piezo, since the electrical short-circuit caused by the spark relaxes the piezo element. With proper mechanical design, the available electrical energy increases to

$$U_e = \frac{1}{2} C_0 V^2. \quad (17)$$

However, the liberation of this additional energy is connected with an acoustic wave that traverses the piezo between the electrode ends when the initial spark discharge occurs. Since the velocity of this acoustic wave is about 4 mm/ $\mu$ s [14], the timescale over which the additional energy is provided is excessively long compared to the typically nanosecond duration of the output pulse from the piezo HVG. This

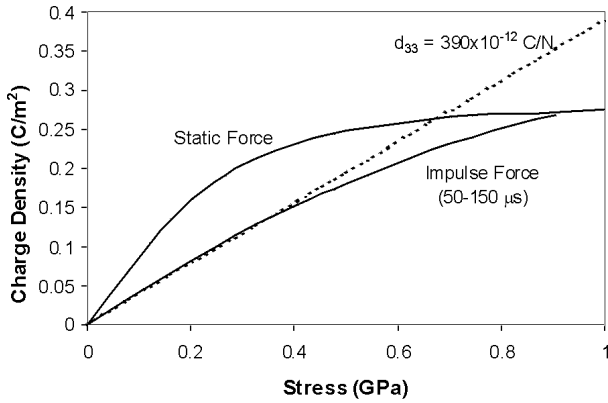


Fig. 2. Equivalent circuit of piezo element with antenna load.

means that the more pessimistic energy calculation of Eq. (15) should be used in practice.

Using a value of 0.69 for  $k_{33}$  from [14], the energy stored in the piezo element for an applied force of 10 kN is 28 mJ. Assuming that a specified compressive stress limit of 600 MPa can be tolerated, the force could be as high as 100 kN. This means an electric energy density of 2.8 J is attainable. This conforms approximately with the maximum energy density of approximately 1.2 J/cm<sup>3</sup> stated in [14].

A case of special interest in terms of applications is shown below in Fig. 2. The capacitive piezo element is connected to a load capacitance  $C_L$ , which together with an inductor  $L$  and a fast spark gap switch could represent a wideband antenna load as shown in Fig. 2. There are two parameters of interest. The first is the maximum voltage that can be achieved on the load, and the second is the number of times the load could be recharged before the piezo element is irreversibly depolarized. Note that for quasi-static stressing, the piezo is capable of supplying current to the load for a period long enough to permit spark gap recovery and hence a multiple pulse output. This means that the most of the energy could be extracted from the piezo, even in situations where the load capacitance is too small to extract it in a single pulse. This has significance relative to generating wideband RF pulses, where antenna capacitances are typically small.

From Eqs. (4) and (8), the voltage  $V$  across the piezo and load capacitances is given by

$$V = E_{3l} = -g_{33}T_{3l} - \frac{C_L l}{\epsilon_{33}^T A} V, \quad (18)$$

so that

$$V = -\frac{g_{33}T_{3l}}{1 + \frac{C_L}{C_0}} = \frac{V_{oc}}{1 + \frac{C_L}{C_0}} \quad (19)$$

where  $V_{oc}$  is the open-circuit voltage that would have been obtained without the load. The efficiency  $\eta$  with

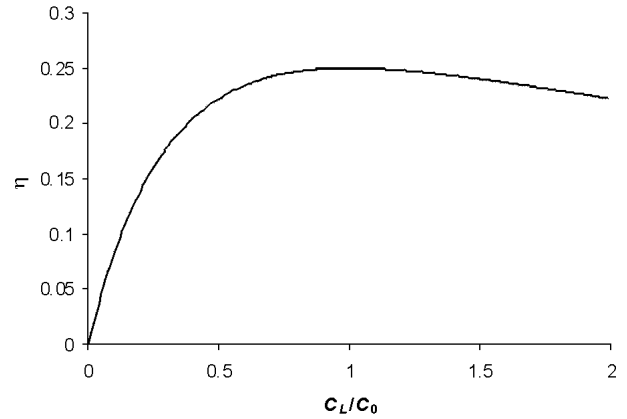


Fig. 3. Piezo charging efficiency vs. load capacitance.

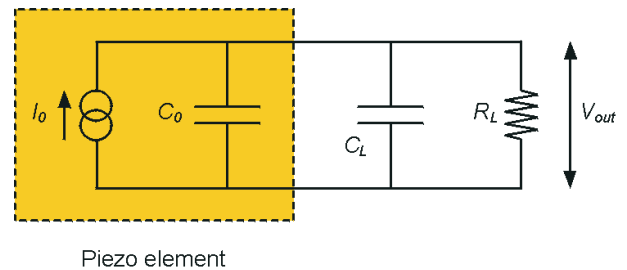


Fig. 4. Quasi-static equivalent circuit of piezo element with  $R - C$  load.

which the piezo energy is transferred to the load is given by

$$\eta = \frac{\frac{1}{2} C_L V^2}{\frac{1}{2} C_0 V_{oc}^2} = \frac{\frac{C_L}{C_0}}{\left(1 + \frac{C_L}{C_0}\right)^2}. \quad (20)$$

Equation (20) is shown graphically in Fig. 3. Note that the maximum charging efficiency is 25 % and occurs when the load and piezo capacitances are equal.

Equations (19) and (20) are derived from the ideal linear theory that does not account for depolarization effects. As discussed previously for the short-circuit load case, the maximum charge density  $D_{max}$  obtainable from PZT-5A is about 0.275 C/m<sup>2</sup>. This means that the output voltage from the piezo for the loaded case must be limited to

$$V \leq \frac{AD_{max}}{C_L} = \frac{Q_{max}}{C_L} \quad (21)$$

where  $A$  is the cross-sectional area of the piezo. If the load capacitance is sufficiently small, then Eq. (21) will be satisfied and the voltage will be limited only by the maximum allowable compression force.

There may be cases where the charge transferred to the load is sufficiently small that multiple charging cycles may be possible during a single compression. When the spark gap fires, it is assumed that the load and piezo capacitances are both discharged.

The charge lost when the spark gap switch closes is therefore

$$Q = (C_0 + C_L)V_{sw}, \quad (22)$$

where  $V_{sw}$  is the voltage at which the switch closes. The total number of recharge cycles that can be provided before the piezo is irreversibly depolarized is therefore

$$N = \frac{AD_{max}}{(C_0 + C_L)V_{sw}}. \quad (23)$$

If the piezo can be prevented from discharging following the switch closure, which could be arranged by using a large resistance between the piezo and the load capacitance, then the number of pulses increases significantly to

$$N = \frac{AD_{max}}{C_L V_{sw}}. \quad (24)$$

If the piezo can be prevented from fully discharging during each switch closure, then a 15 mm, 20 mm long PZT-5A element would, in principle, be capable of recharging a 10 pF load to 100 kV about 50 times before complete depolarization. If the piezo is discharged at every switch closure, then the number of pulses is about 3.

Using the simple theory discussed in this section, it is possible to relate the results of basic measurements of the piezo characteristics to the obtainable output voltage in a piezo-based HVG. These measurements are discussed in Section 3.

### 3. Results and Discussion

In order to verify the theory discussed in Section 2, quasi-static measurements of a 15 mm diameter, 20 mm long cylindrical PZT-5A piezo element were conducted using an electric press driven by a rotating screw. This system is capable of producing approximately sinusoidal stresses up to 200 kN with a frequency approaching 1 Hz for small stresses and about 30 seconds for longer stresses. The maximum frequency decreases as the maximum stress increases. Strain gauges were fixed to the side of the piezo with adhesive. Both axial and radial strain could be measured with these gauges.

The equivalent circuit for the piezo element under quasi-static conditions is shown in Fig. 4. The piezo can be represented as a current source connected across a fixed capacitance  $C_0$ , which was both calculated and measured to be 135 pF. The piezo is then connected to a load which can have either resistive ( $R_L$ ) or capacitive ( $C_L$ ) components. For these experiments, a resistive probe with an input impedance of 100 M $\Omega$  was constructed using 10  $\times$  10 M $\Omega$  resistors connected in series. At the ground end of the resistor chain there was a 100 k $\Omega$  resistor. This probe could either be used as a high-impedance current probe for static testing, where 100 M $\Omega$  is

effectively a short-circuit, or as a voltage probe for dynamic stress piezo testing.

The current through the piezo can be determined from the measured voltage  $V_{out}$  by using

$$I_0(t) = \frac{V_{out}}{R_L} + (C_0 + C_L) \frac{dV_{out}}{dt}. \quad (25)$$

In addition, the open-circuit (unloaded) voltage produced by the piezo can be determined from

$$V_{oc}(t) = \left(1 + \frac{C_L}{C_0}\right) V_{out} + \frac{1}{R_L C_0} \int_0^t V_{out}(t') dt'. \quad (26)$$

For quasi-static testing, the open-circuit voltage is difficult to measure directly, since the measurement time constant  $\tau = R_L C_0$  must be considerably longer than the time over which the force is applied. If  $C_0$  is 135 pF, this means that the input impedance of the measurement probe must be on the order of 10 G $\Omega$ . This is clearly unrealistic. The two practical options are to measure the output current  $V_{out}/R_L$  and then reconstruct the open-circuit voltage using Eq. (26) or to use a capacitor  $C_L$  of 10–100 nF with a realistic voltage probe resistance  $R_L$  of 100 M $\Omega$  to provide a suitable measurement time constant  $\tau$ . In this case, the probe will be self-integrating. With either method, to determine the open-circuit output voltage requires a reliable value of  $C_0$  and confirmation of the validity of the equivalent circuit shown in Fig. 4.

To check both the value of  $C_0$  and the validity of the circuit model, a preliminary dynamic stress test of the piezo element was performed. The piezo element was installed inside a PVC tube. An 18.25 mm diameter steel ball bearing was dropped onto the piezo from a height of 190 mm by withdrawing a pin from under the bearing. When the bearing struck a small steel cylinder placed on top of the piezo, an impulsive stress with a FWHM of about 20  $\mu$ s was generated. Because of the short duration of the stress, the 100 M $\Omega$  voltage probe was self-integrating and the open-circuit output voltage could be measured directly. A number of different capacitive loads were connected across the output of the piezo and the output voltage measured. Since the stress generated by the falling ball bearing was repeatable, from Eq. (26) the measured output voltage in the loaded cases should be related to the open-circuit voltage by

$$V_{oc}(t) = \left(1 + \frac{C_L}{C_0}\right) V_{out}. \quad (27)$$

The measured output voltages for the dynamic stress test for various load capacitances  $C_L$  are shown in Fig. 5. A peak open-circuit voltage of about 4 kV was measured, with the voltage decreasing for increasing load capacitance, as expected from Eq. (27).

The peak output voltage  $V_p$  was determined and its inverse plotted against load capacitance as shown

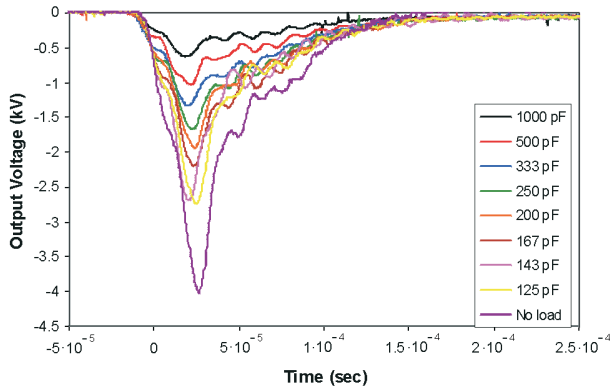


Fig. 5. Measured piezo output voltages from dynamic stress test.

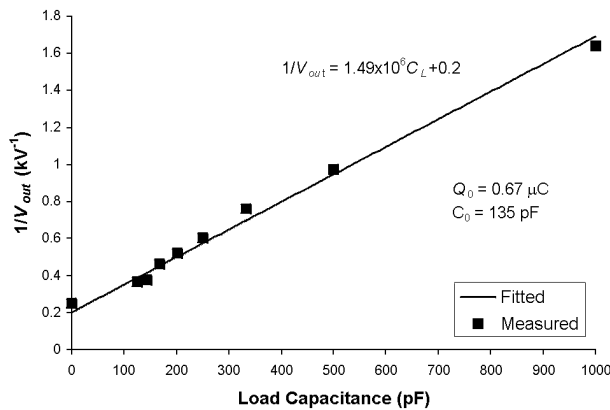


Fig. 6. Maximum piezo output voltages plotted against load capacitance for dynamic stress.

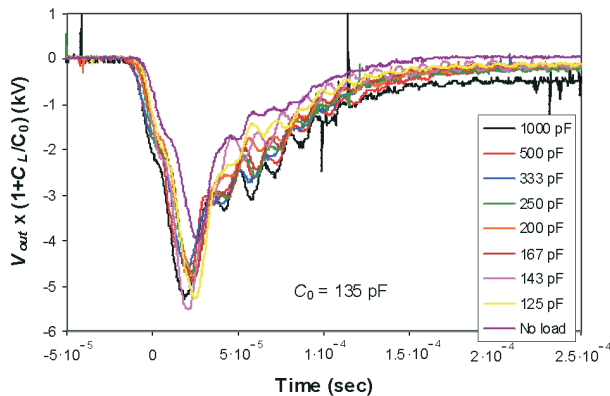


Fig. 7. Rescaled piezo output voltages for dynamic stress test.

in Fig. 6. From Eq. (27),

$$\frac{1}{V_p} = \frac{C_0}{Q_0} + \frac{C_L}{Q_0}, \quad (28)$$

where  $Q_0 = C_0 V_p$  is the maximum charge produced by the piezo element. Using the value for  $C_0$  of 135 pF, which was calculated in Section 2.1, and confirmed by low-voltage bridge measurements,  $Q_0$  was determined to be 0.67  $\mu\text{C}$ , using a least squares fit. The reasonable

quality of the fit shown in Figure 6 also serves to verify the equivalent circuit shown in Fig. 4, although further verification was considered necessary.

Figure 7 shows the measured output voltages shown in Fig. 5 rescaled according to Eq. (27). Since the open-circuit voltage  $V_{oc}$  should be the same for any load capacitance, the rescaled waveforms should ideally be identical. In practice, because the integral term in Eq. (25) has been ignored in the derivation of Eq. (27), the output voltage for small capacitive loads, particularly at late times, will be slightly underestimated. In addition, it is reasonable to assume stray capacitance will also act to reduce the output voltage slightly for small or zero external load capacitances. Regardless of this, the reasonable agreement indicated in Fig. 6 indicates that the conclusions regarding the piezo capacitance  $C_0$  and the validity of the circuit model obtained from the measurement of the peak voltage are generally applicable to the entire range of output voltage waveforms.

With confidence in the value of  $C_0$  and the validity of the equivalent circuit model, the quasi-static testing of the piezo element could proceed. The first test was to measure the output current with a number of resistive loads ranging from 17 to 100  $\text{M}\Omega$ . The piezo was subjected to an approximately sinusoidal force ranging from 0 to 5 kN with a period of about 2.5 seconds. This equates to a stress of 28 MPa. If the circuit model is correct, the output current should be the same, regardless of the load resistance. The results of this test are shown in Fig. 8. The repeatability is excellent, showing that the piezo current is unaffected by load resistances over this range.

For the next quasi-static test, the effect of varying the load capacitance with quasi-static stressing was investigated. The load resistance in this case was simply the current probe resistance of 100  $\text{M}\Omega$ . The measured voltage from the probe for a variety of load capacitances  $C_L$  is shown in Fig. 9. As for the previous quasi-static test, a force varying approximately sinusoidally between 0 and 5 kN with a period of 2.5 seconds was applied to the piezo. Although the measured voltage is very dependent on the load capacitance, applying Eq. (26) to eliminate the probe response shows that the variation is due to the effect upon the probe measurement. As Fig. 10 shows, the piezo open-circuit voltage is relatively independent of the load capacitance, as expected from the equivalent circuit model. A peak voltage of between 15 and 20 kV is implied from this measurement. This corresponds to a charge of 2–2.7  $\mu\text{C}$ .

In principle, it is possible to increase the output of a piezo HVG by stacking a number of piezo elements in series. According to the circuit model, the current through the piezo stack should be the same as for each individual piezo; however, the total capacitance  $C_{stack}$

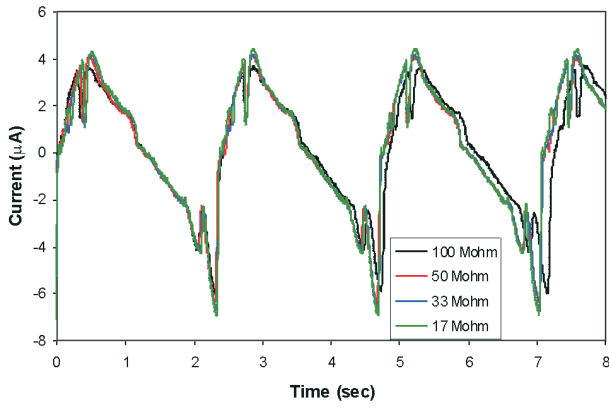


Fig. 8. Piezo output current for various load resistances and quasi-static stresses.

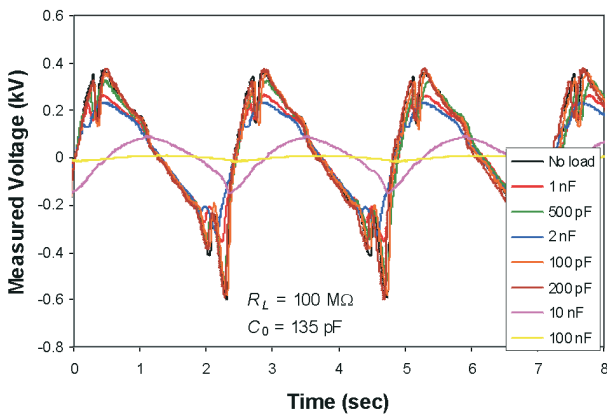


Fig. 9. Piezo output voltages for various load capacitances and quasi-static stresses.

of the piezo stack will be

$$C_{stack} = \frac{C_0}{N}, \quad (29)$$

where  $N$  is the number of piezos. The open-circuit voltage will therefore be proportional to  $N$ . This means that, in principle, any voltage can be achieved by a stacking a suitable number of piezo elements, although the total capacitance of the piezo stack does decrease as the number of piezo elements increases. To check this principle, three piezos were stacked in series and mounted in the press. The currents measured through the bottom piezo element, the lower two piezo elements and the complete stack is shown in Fig. 11. As expected from the theory, the current is the same in all cases. This shows that series stacking can be exploited to produce higher voltages. Note that piezo elements can also be stacked in parallel for driving high-capacitance loads; however, in practice, high-power antennas are low-capacitance loads, so that achieving a higher voltage is normally the priority.

Once the validity of the circuit model had been demonstrated, the next step was to subject the piezo to various load stresses and measure the output

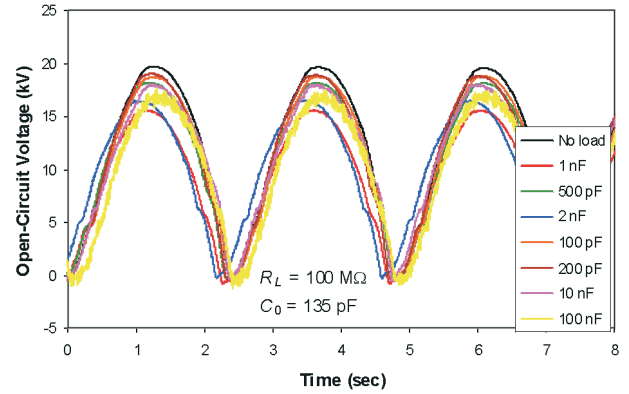


Fig. 10. Piezo open-circuit voltages for various load capacitances.

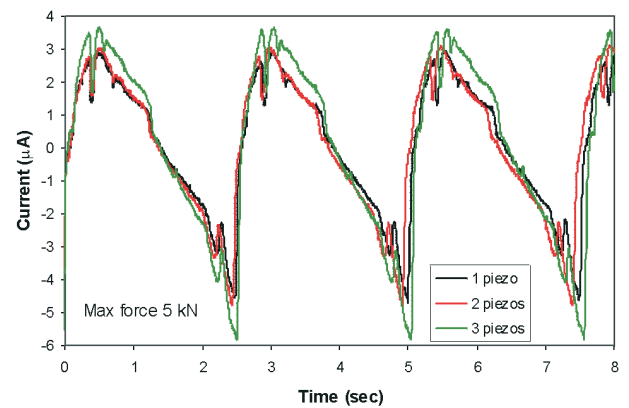


Fig. 11. Current through series piezo stack.

current. From the circuit model, the corresponding open-circuit voltage could be determined. The intention of these experiments was to verify the calculations in Section 2 and to examine the effects of depolarization at higher stress levels. Figure 12 shows the applied force and the total charge obtained from the piezo determined from integrating the measured output current for various amplitudes of the applied force. Note that, in principle, the open-circuit voltage can be calculated simply by dividing the charge by the piezo capacitance of 135 pF. This means that the maximum voltages for the 5,10,15, and 20 kN maximum force tests were 22,58,88, and 72 kV, respectively.

Using the data shown in Fig. 12, the piezo open-circuit voltage is plotted against the applied force in Fig. 13 for each of the four cases shown in Fig. 12. Several interesting features are apparent. The first is that the charge produced by the piezo for the lower maximum forces of 5 and 10 kN is somewhat higher than predicted from the linear theory discussed in Section 2, in particular Eq. (12). This is consistent with Figure 1, reproduced from [14], which shows that the nonlinear piezoelectric effect accompanying static stressing produces significantly higher charge from the piezo than anticipated from the linear theory. The

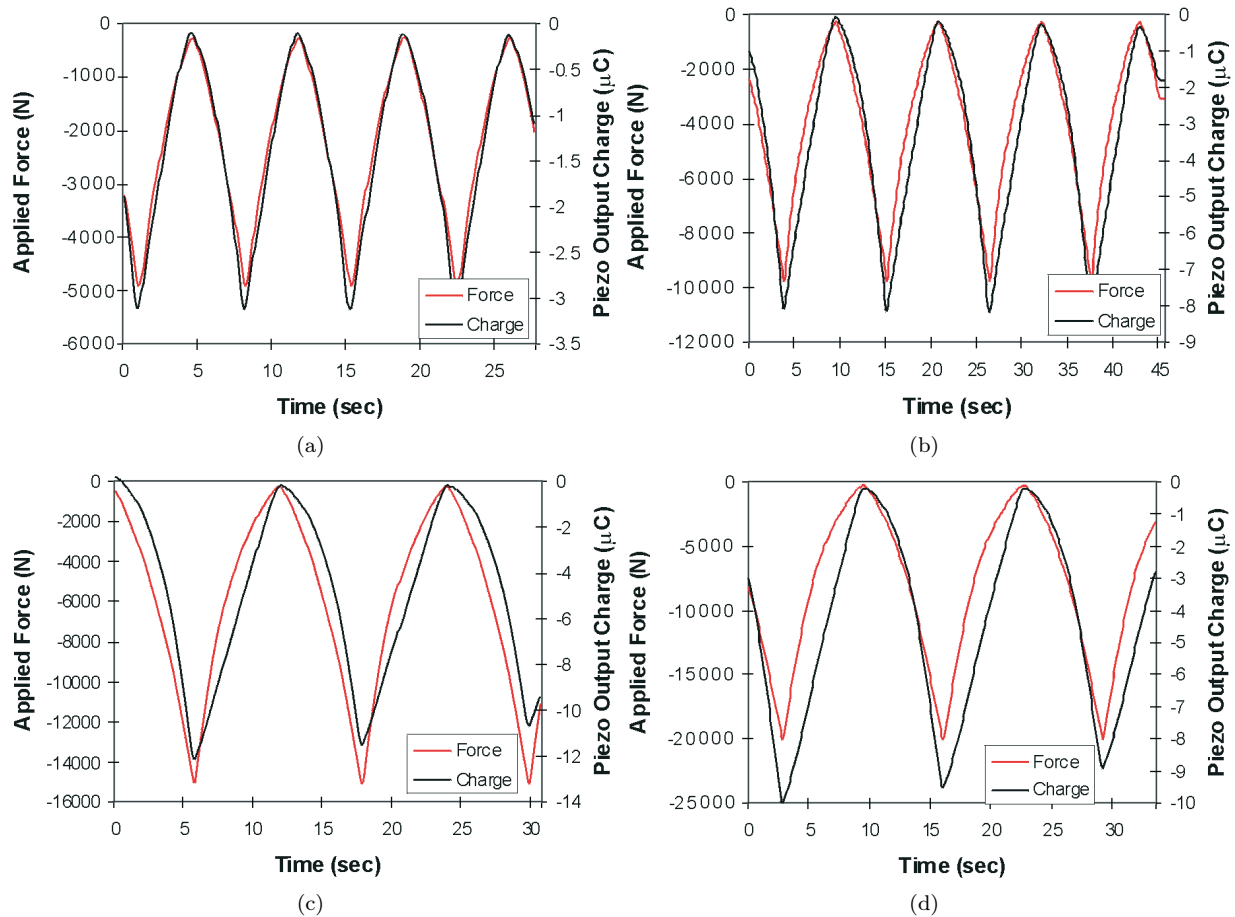


Fig. 12. Measured force and piezo output charge for forces of 5,10,15, and 20 kN.

discrepancy between the theory and the measurements is therefore to be expected. The second interesting observation is that the charge delivered from the piezo noticeably decreases during successive stress cycles for the 15 and 20 kN maximum stress tests. This is also apparent from Fig. 12 and indicates that depolarization of the piezo is occurring. Note that the same piezo element was used to obtain all of the data in Figs. 12 and 13. This successive depolarization explains why the maximum charge for the 20 kN maximum stress case is less than the charge obtained during the 15 kN maximum stress test performed earlier. The decreasing open circuit voltage meant that there was good reason to believe that using a new piezo element for each test and recording data starting from the first compression would show a significant increase in the charge delivered by the piezo.

Figure 14 shows the total charge delivered by the piezo with quasi-static compression for maximum forces of 10,20, and 50 kN. The piezo output current was recorded from the start of the compression and new piezos were used for each test. As for the data in Fig. 12, the period of one compression cycle is about 10 seconds for a 20 kN maximum force, increasing to 30 seconds for a 50 kN force. A test was also performed to determine the maximum static stress that the piezo

element could withstand using a maximum force of 200 kN available from the press. Data was recorded over a 100 second time window.

The results shown in Fig. 14 show that even at a low force of 10 kN, depolarization effects are significant. The first compression cycle produced significantly more charge than subsequent cycles. With a 10 kN maximum force, the depolarization process stabilized after the first compression cycle and the results are similar to those presented in Figs. 12 and 13 for a 10 kN force. For 20 kN and 50 kN maximum forces, the depolarization effect is much more severe. This indicates that a force of not more than 10 kN should be used if reasonable charge is to be drawn repetitively from the piezo. On the other hand, for single shot applications, it is clear that much greater charge can be extracted with higher stress. The maximum charge produced with 10, 20 and 50 kN maximum force was 13,32.5 and 49  $\mu\text{C}$ , respectively. Note that the approximate limit of  $0.275 \text{ C/m}^2$  shown in Figure 1 corresponds to 49  $\mu\text{C}$  for a 15 mm diameter piezo element, indicating that the piezo element has been almost completely depolarized with a 50 kN maximum force. This is verified by the plot on the lower right of Figure 14 corresponding to the break test. At approximately

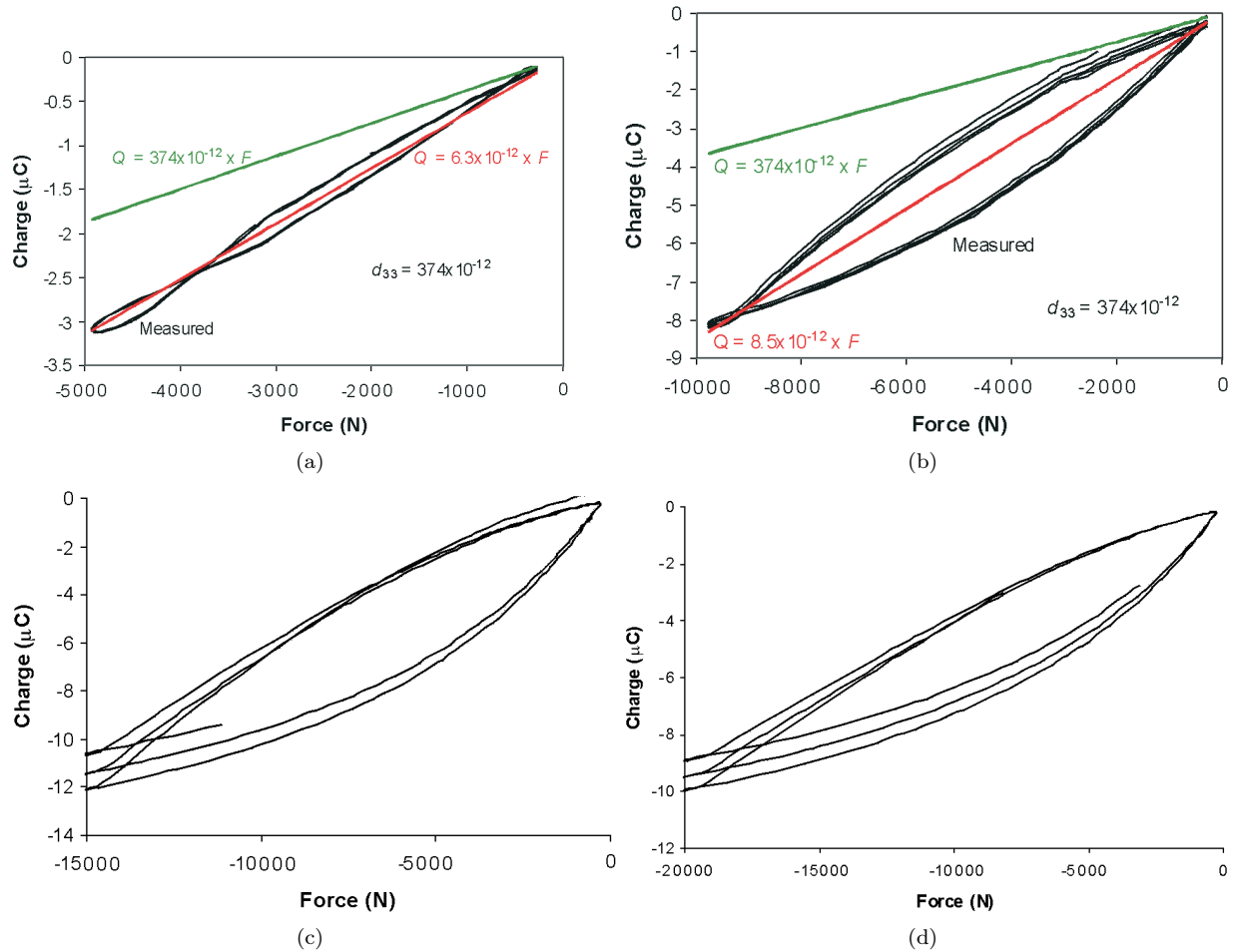


Fig. 13. Piezo output charge plotted against force (5,10,15, and 20 kN max).

125 kN, corresponding to a stress of 700 MPa, the piezo element shattered completely. From Eq. (14), this corresponds to a maximum open-circuit voltage of approximately 330 kV. This stress limit is consistent with the figure of  $> 600$  MPa stated in [2]. The piezo is clearly significantly depolarized after 40 kN has been applied and has been almost completely discharged by about 60 kN.

A maximum available charge greater than  $50 \mu\text{C}$  is sufficient to charge even a relatively high-capacitance 150 pF load to 330 kV. This means that in practice, the maximum voltage produced by the piezo will be limited by the maximum possible force that can be applied before the piezo shatters, rather than the available charge. In other words, the maximum single-pulse voltage is limited according to Eq. (25), rather than by the available charge, as stated by Eq. (26). An additional factor is that in a practical HVGs, the piezo must be insulated to prevent not only breakdown, but also leakage current from discharging it. It is unlikely that a voltage exceeding 330 kV could be maintained across a single piezo element only 20 mm long. Therefore, in practice, the voltage capability of

the piezo element for single-shot applications is almost certainly limited by the insulation in the HVG and not by a fundamental limitation of the piezo itself.

Note that the capacitance of the piezo elements used to obtain the results presented in Fig. 14 was measured following the tests. The capacitance of all three is in the range 130–145 pF. This means that depolarization was not accompanied by a variation in the unstressed capacitance value.

A strain gauge fixed to the side of the piezo was used to measure the longitudinal strain against the applied force. The most useful is the strain measurement for the overstress test where the piezo was tested to destruction. The result of this measurement is shown in Fig. 15. Also shown is the theoretical relationship represented by Eq. (12). At very low stress, the theoretical and experimental results agree. As the stress increases, the strain increases faster than predicted due to the nonlinear piezoelectric effect discussed previously, which also produces more than the predicted amount of charge. Due to the electromechanical coupling within the piezo, it is not surprising that an effect which affects the amount of charge delivered by the piezo should

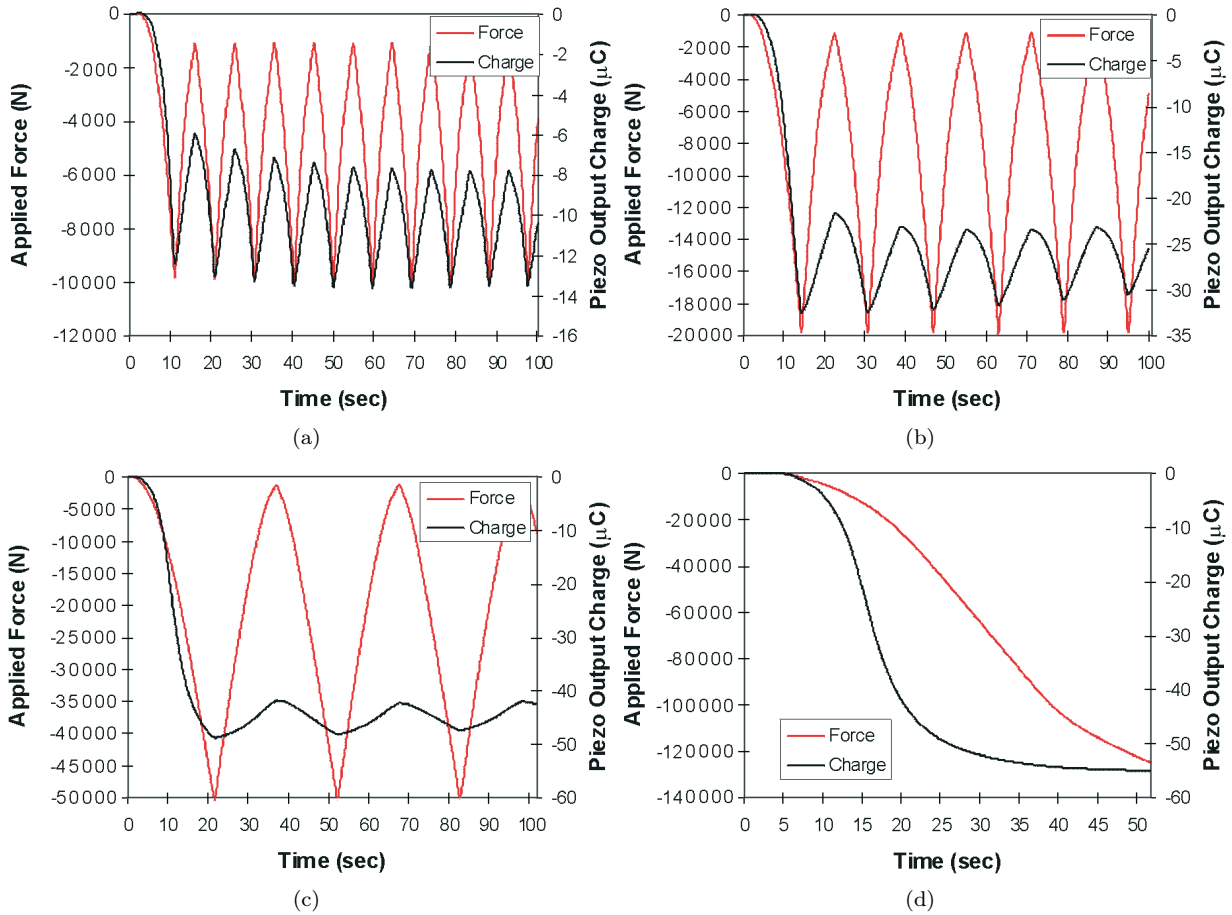


Fig. 14. Measured forces and piezo output charges for applied forces of 10,20,50, and 200 kN.

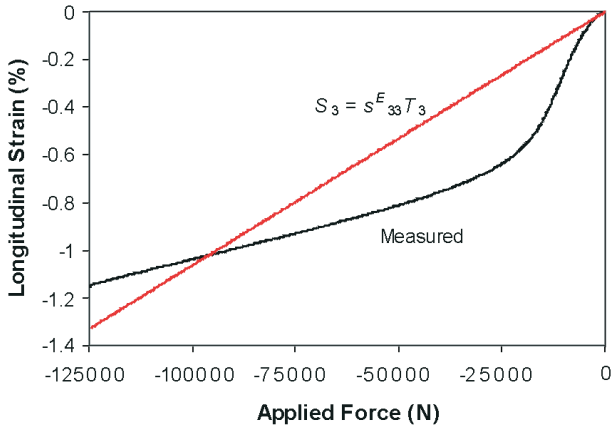


Fig. 15. Strain against applied force.

also affect the mechanical characteristics. As the force increases beyond about 40 kN, the piezo becomes depolarized and becomes harder, in that further increasing the stress produces a negligible increase in the strain. A maximum strain of about 1 % was produced, corresponding to 0.2 mm in the 20 mm piezo element.

The results presented in this section show that in principle, quasi-static compression of PZT-5A

piezo elements can be exploited to produce voltages on the order of 100–1000 kV in compact high-voltage generators. Operation can be either single-shot or repetitive, although the attainable voltage in repetitive systems is significantly lower. A total charge of about 50  $\mu\text{C}$  is available with an applied force of 40 kN from the 15 mm diameter, 20 mm long piezo elements used during the tests described in this section. This is more than adequate to charge low-capacitance impulse antennas to voltages of more than 100 kV. It was concluded from these results that a high-voltage generator exploiting simple quasi-static stressing of the piezo elements was capable of meeting the requirements for a compact high-power RF source. More mechanically complicated schemes based on dynamic stressing of the piezo, or explosively generated shock waves, are not required.

#### 4. Conclusions

The results presented in this paper show that a compact HVG based on piezo elements is feasible. Tests have shown that simple quasi-static compression of the piezo elements is adequate to charge a low-capacitance load such as a wideband antenna

for generating high-power RF radiation. Charging voltages in the range 100–1000 kV are possible based on the charging scheme and the number of piezos used. The main limitation on the achievable antenna charging voltage will be electrical breakdown either inside or along the exterior of the antenna, rather than a limitation of the piezo. For this reason, more complicated schemes such as shock depolarization or dynamic compression of the piezo elements are not warranted.

Manuscript received August 1, 2003

## References

- [1] Neilson F.W. Ferromagnetic and Ferroelectric One-Shot Explosive Electric Transducers // S.C.T.M. – V. 230B. – P. 56–61.
- [2] Neilson F.W. and Anderson G.W. // Bull. Am. Phys. Soc. – 1957. – V. 11(2). – P. 302.
- [3] R.H. Wittekindt, "Shape of the Current Output Pulse from a Thin Ferroelectric Cylinder under Shock Compression", D.O.F.L., TR., p. 922 (1966).
- [4] Reynolds C.E. and Say G.E. Two-Wave Shock Structures in the Ferroelectric Ceramics: Barium Titanate and Lead Zirconate Titanate // J. Appl. Phys. – 1962. – V. 33. – P. 2234.
- [5] Rose M.F. and Massie J.A. // U.S. Patent 4.090.448.
- [6] Novitsky E.Z., Sadunov V.D. and Karpenko G.I. // Physics of Combustion and Explosion (in Russian). – 1972. – V. 14. – P. 115.
- [7] Mineev V.N. and Ivanov A.G. EMF Formed during Shock Compression of Matter // Proc. Of the Conference on Megagauss Magnetic Field Generation by Explosives and Related Experiments, Euroatom. – 1976. – P. 317.
- [8] Besancon J.E., David J., and Vedel J. Ferroelectric Transducers // Proceedings of the Conference on Megagauss Magnetic Field Generation by Explosives and Related Experiments (eds. H. Knoepfel and F. Herlach), Euratom, Brussels. – 1966. – P. 315–328.
- [9] Prishchepenko A.B., Ttretyakov D.V., and Shchelkachev M.V. Energy Balance In Frequency Explosive Piezoelectric Generator During Its Operation // Megagauss And Megaampere Pulse Technology And Applications, Proceedings of 7th International Conference on Megagauss Magnetic Field Generation and Related Topics (Eds. V.K. Chernyshev, V.D. Selemir & L.N. Pljashkevich). – Sarov (Arzamas-16), – August 5-10, 1996. – Part 2, P. 925–928.
- [10] Ludu A., Nicolau P., and Novac B., Shock Wave-Explosive Energy Generation of PZT Ferroelectric Ceramics, Megagauss Technology and Pulsed Power Applications (eds. C.M. Fowler, R.S. Caird, and D.J. Erickson). – New York: Plenum Press., – 1986. – P. 369–376.
- [11] Shkuratov S.I., Kristiansen M., Dickens J., Neuber A., Altgilbers L., Tracy P.T., and Tkach Ya. Experimental Study of Compact Explosive Driven Shock Wave Ferroelectric Generators // Tenth HPM Conference, Washington DC. – April 3–5, 2001.
- [12] Tkach Ya., Shkuratov S., Talentsev E.F., Dickens J.C., Kristiansen M., Altgilbers L.L., and Tracy P.T., Theoretical Treatment of Explosive-Driven Ferroelectric Generators // IEEE Transactions on Plasma Science. – 2002. – V. 30(5). – P. 1665–1673.
- [13] "Properties of Piezo Material Lead Zirconate Titanate", efunda Engineering Fundamentals Web Site.
- [14] Koch J. Piezoxide (PXE) Eigenschaften und Anwendungen, Dr Alfred Huthig Verlag GmbH, ISBN 3-7785-1755-4, 1988.